Physica B 185 (1993) 239–244
North-Holland

PHYSICA B

Magneto-optics of Cu-related defects in polymorphic ZnS

P. Thurian, R. Heitz, T. Jentzsch, A. Hoffmann and I. Broser
Institut für Festkörperphysik, Technische Universität, Berlin, Germany

High-resolution spectroscopy of weakly Cu-doped polymorphic ZnS crystals leads to the detection of new $Cu_{Zn}^{2+}(^2E-^2T_2)$ zero-phonon lines in the 0.86 eV spectral region. As a result of Zeeman measurements a general classification scheme for the different lattice sites of the Cu_{Zn}^{2+} centres is presented. The axially distorted Cu_{Zn}^{2+} impurities show an anisotropical Zeeman pattern and a zero field splitting in the excited ^2E-states. The order of magnitude of the g values indicates a strong Jahn–Teller interaction in the $^2T_2$-ground state.

1. Introduction

Copper is an efficient luminescence activator in II–VI compounds. At least four prominent Cu-related luminescence bands (Cu-infrared, Cu-red, Cu-green and Cu-blue) are known in ZnS [1]. The Cu-infrared band is attributed to a Cu_{Zn}^{2+} intrashell $^2E-^2T_2$ transition [2], whereas the physical origin of the blue emission band is controversially discussed hitherto [3,4]. It is the purpose of this paper to present a detailed magnetooptical investigation of the Cu-infrared zero-phonon lines (ZPLs) at 0.86 eV in polymorphic ZnS crystals. As a result of this a general classification scheme for the different lattice sites of the Cu_{Zn}^{2+} centres in polymorphic ZnS is derived. Finally, it is demonstrated that no Cu_{Zn}^{2+} states are involved with the blue emission band.

2. Experimental results

All modifications of ZnS consist of sequences of Zn–S layers being stacked along the $(1\,1\,1)_g$ direction of growth. Transition metal (TM) impurities substituting Zn^{2+} ions are located in a tetrahedrally coordinated S^{2-} environment, which belongs to two Zn–S layers. Thus, four different lattice sites exist for a substitutional impurity if the possible arrangements of the Zn–S layers above and below these two layers are considered. The four sites are called AN (cubic), (AS, PN) (axially distorted), and PS (hexagonal) [5]. P indicates a prismatic, A an antiprismatic coordination, S the existence of a single third neighbour on the stacking axis, N its absence.

In this contribution we consider six Zn–S layers, which leads to a classification scheme [6] of 16 different lattice sites for the substitutional Cu_{Zn}^{2+} impurity. The ZnS single crystals are grown by the Broser–Warminsky method [7] and are subsequently doped in the ppm region by diffusion of copper. They contain also nickel, tungsten and iron as unintentional dopants. Exciting these crystals in the charge transfer band of Cu_{Zn}^{2+} at 2.50 eV, the Cu-IR photoluminescence (PL) is observed. A detailed investigation of the Cu^{2+} excitation mechanism in II–VI compounds is described in [8].

2.1. Fine structure of the Cu_{Zn}^{2+} centres

The tenfold degeneracy of the ^2D term of the Cu^{2+} (d^9-system) is lifted by a tetrahedral (T_d) crystal field into a $^2T_2$ sextuplet (ground-state) and a ^2E quadruplet (excited state). The spin–orbit interaction further splits the $^2T_2$ ground-state into a Γ_7 doublet and a Γ_8 quadruplet. The ^2E level becomes a Γ_8 state. A trigonal (C_{3V})

Correspondence to: P. Thurian, Institut für Festkörperphysik, Technische Universität Berlin, PN5-3, Hardenbergstrasse 36, 1000 Berlin 12, Germany.

crystal field, caused by the wurtzite crystal structure or a stacking fault, splits the Γ_8 states into a Γ_4 and a $\Gamma_{5,6}$ Kramers doublet, respectively. The Γ_7 state becomes a Γ_4 state. The magnitude of the $\Gamma_8(^2E)$ zero field splitting (ZFS) is given by the parameter D. The different trigonal field in polymorphic ZnS enables us to compare the fine structure of Cu_{Zn}^{2+} centres in slightly different environments.

The ZPL region of the $Cu_{Zn}^{2+}(^2E-^2T_2)$ PL in different polymorphic ZnS crystals is shown in fig. 1. The cubic (99%) crystal (a) exhibits two ZPLs, whereas the spectra of the polymorphic crystals (b–c) show several new ZPLs. These ZPLs are attributed to transitions within different axial distorted Cu_{Zn}^{2+} centres as shown below.

Cubic centres AN, AN3. Unpolarized ZPLs of the cubic AN and AN3 centres are shown in fig. 2 with high resolution. They are attributed to the $\Gamma_8(^2E)-\Gamma_7(^2T_2)$ transition: The unpolarized ZPL at 856.78 meV was tentatively attributed to the $\Gamma_8(^2E)-\Gamma_8(^2T_2)$ transition of the AN centre [9]. The order of magnitude of the $^2T_2$ ground state splitting calls for a strong Jahn–Teller effect reducing the spin–orbit splitting constant. The intensity of the cubic AN ZPLs is independent from the intensity of the other Cu_{Zn}^{2+} ZPLs. It

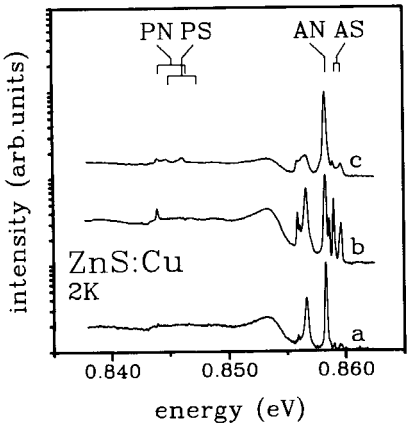

Fig. 1. Cu_{Zn}^{2+} PL spectra of three ZnS single crystals containing different polytypic parts. Crystal a is almost cubic, whereas for b and c the polytypic parts are increased. The zero field splittings (ZFS) D in the excited ^{2}E-states and the centre of gravity for the AN, AS, PN and PS centre are indicated.

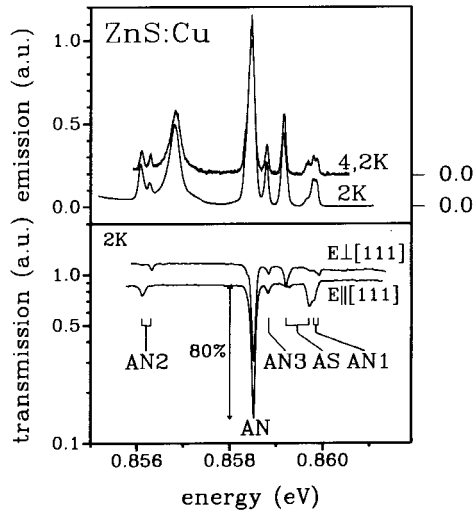

Fig. 2. Emission and polarized absorption spectra in the energy range of the cubic AN ZPLs at $T = 2$ K and $T = 4.2$ K (crystal b, fig. 1). The assignments of the different ZPLs to the corresponding defect centres and the zero-field splitting in the excited ^{2}E state are indicated.

should be noticed that the change of the intensity ratio between the 858.46 meV AN ZPL and the vibronic sideband (fig. 1) is caused by reabsorption of the AN ZPL luminescence. The reabsorption depends on the Cu^{2+}/Cu^{+} ratio in the illuminated crystal.

Axial centres AN1, AN2, AS, PN and PS. The three polarized ZPL pairs, labeled AN1, AN2 and AS in fig. 2, show a thermalization in PL. This is caused by a ZFS in the excited ^{2}E-states of these defect centres. We obtain $D = 0.08$, 0.20 and 0.51 meV for the AN1, AN2 and AS centres. In comparison with these axial centres the magnitude of the ZFS for the PN and the PS centre is increased to 2.45 meV and 2.43 meV, respectively. The intensity between the (AN1 : AN2) ZPLs as well as the (PN : AS) ZPLs has a ratio of 1 : 1, whereas the intensity of the PS ZPL is independent (fig. 1). It should be mentioned, that the sign of the ^{2}E splitting parameter D is the same for the PN, PS, AN1 and AN2 centres, whereas for the AS centres a reversed sign is observed. The energy positions and the symmetries of the states for all observed Cu_{Zn}^{2+} centres are summarized in table 1.

Table 1
The energy differences, the term symmetries, the zero-field splitting parameter D and the observed g values for the different Cu^{2+}_{Zn} centres in polymorphic ZnS. The $g_{\perp}$ values of the ^2E state for the AN1, AN2 and AS centres are obtained with the equation $\Delta E = (D^2 + (\mu_B g_{\perp} B^2))^{1/2}$. The energy shifts ΔE of the centre of gravity for the AS, PN and PS centres to the cubic AN centre are also given.

Cu^{2+} state	Energy (meV)	D (meV)	g value $H \perp (1\,1\,1)$	g value $H \parallel (1\,1\,1)$	ΔE(AN) (meV)	Centre
$\Gamma_8(^2E)$	858.46	0	1.69 ± 0.01	1.67 ± 0.01	0	AN
$\Gamma_8(^2T_2)$	1.68		0.96 ± 0.15	0.96 ± 0.15		
$\Gamma_7(^2T_2)$	0		0.61 ± 0.02	0.62 ± 0.02		
$\Gamma_8(^2E)$	858.78	0	1.69 ± 0.03	1.68 ± 0.05	0.32	AN3
$\Gamma_7(^2T_2)$	0		0.61 ± 0.02	0.61 ± 0.02		
$\Gamma_{5,6}(^2E)$	859.85	0.08	1.49 ± 0.08	1.53 ± 0.08	1.35	AN1
$\Gamma_4(^2E)$	859.77			1.53 ± 0.08		
$\Gamma_4(^2T_2)$	0		0.56 ± 0.05	0.79 ± 0.05		
$\Gamma_{5,6}(^2E)$	856.27	0.20	1.67 ± 0.02	1.51 ± 0.04	−2.29	AN2
$\Gamma_4(^2E)$	856.07			1.51 ± 0.04		
$\Gamma_4(^2T_2)$	0		0.41 ± 0.05	0.97 ± 0.09		
$\Gamma_4(^2E)$	859.61	0.51	1.64 ± 0.02	1.45 ± 0.02	0.895	AS
$\Gamma_{5,6}(^2E)$	859.10			1.45 ± 0.02		
$\Gamma_4(^2T_2)$	0		0.29 ± 0.02	1.45 ± 0.02		
$\Gamma_{5,6}(^2E)$	846.56	2.45			−13.155	PN
$\Gamma_4(^2E)$	844.08			1.71 ± 0.02		
$\Gamma_4(^2T_2)$	0		0.28 ± 0.03	1.35 ± 0.05		
$\Gamma_{5,6}(^2E)$	847.27	2.43			−12.40	PS
$\Gamma_4(^2E)$	844.84					
$\Gamma_4(^2T_2)$	0					

2.2. Zeeman behaviour of the Cu^{2+}_{Zn} centres

In the following section the Zeeman behaviour of the different ZPLs is presented. The observed thermalization of the ZPLs allows to distinguish between splittings in the excited and in the ground state for a given ZPL. The symmetry of the states is determined by the observed polarizations.

The Zeeman splitting of the different Cu^{2+}_{Zn} centres can be classified by the trigonal ZFS: the Zeeman pattern is isotropical without ZFS and anisotropical with a ZFS.

Cubic centres AN, AN3. Fig. 3 shows the Zeeman pattern of all ZPLs from fig. 2 for the configuration $H \parallel (1\,1\,1)$ and $H \perp (1\,1\,1)$. The cubic AN ZPL and the AN3 ZPL exhibit an

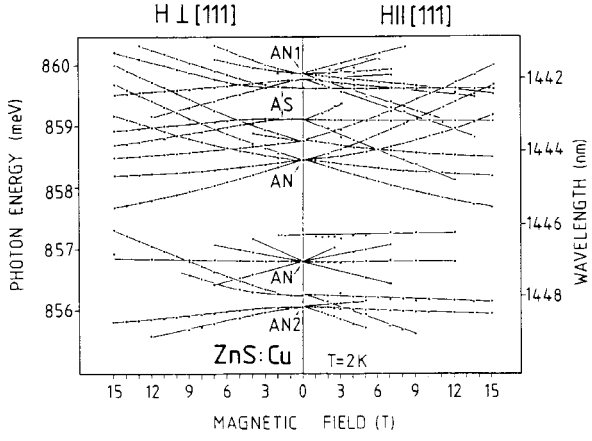

Fig. 3. Zeeman-pattern of the Cu^{2+}_{Zn} ZPLs (fig. 2) for $H \parallel (1\,1\,1)$ (right) and $H \perp (1\,1\,1)$, $H \parallel (1\,1\,0)$ (left) for T = 2 K. The assignments of the different ZPLs to the corresponding defect centres are also given.

isotropical fourfold splitting caused by twofold splittings of both the $\Gamma_7(^2T_2)$ ground state and the $\Gamma_8(^2E)$ excited state. The observed g value of the $\Gamma_8(^2E)$ excited state agrees with the reported [10] one. However, the g value ($g = 0.61$) of the $\Gamma_7(^2T_2)$ ground state is smaller than the reported one of about $g = 0.71$. It is remarkable that the centre of gravity of the 4 ZPLs of the cubic centres is shifted to higher energies with increasing magnetic field. The $\Gamma_8(^2E)$–$\Gamma_8(^2T_2)$ AN emission at 856.78 meV shows a fourfold Zeeman splitting, caused by twofold splittings of the $\Gamma_8(^2E)$ and the $\Gamma_8(^2T_2)$ state.

Axial centres AN1, AN2, AS. The trigonal splittings of the axial centres are small compared with the Zeeman splitting above 10 T, a transition from the weak to the strong magnetic field regime is observed in both configurations (figs. 3, 5).

$H \parallel (1\,1\,1)_g$. All ZPLs show a linear fourfold splitting for $H \parallel (1\,1\,1)$ caused by a twofold splitting of all Kramers doublets involved. The g-values are found to be different for the axial centres. A remarkable trend is observed (table 1): the g values of the excited $\Gamma_4(^2E)$ and $\Gamma_{5,6}(^2E)$, states agree for each single centre and decrease with increasing trigonal ZFS. No degeneracy remains in contrast to the cubic AN centre. Furthermore, the g values in the $\Gamma_4(^2T_2)$ ground states increase from $g = 0.79$ for the AN1 centre up to $g = 1.45$ for the AS centre.

$H \perp (1\,1\,1)_g$, $H \parallel (1\,1\,0)$. In this configuration all ZPLs split just twofold, due to the splitting of the $\Gamma_4(^2T_2)$ ground states. The nonlinear Zeeman behaviour is caused by terminteraction in the excited ^2E state (fig. 5): the two $\Gamma_{3,4}(^2E)$ states shift nonlinearly to higher and lower energies, respectively. The energy splitting ΔE of the ^2E state in a magnetic field is given by $\Delta E = (D^2 + (\mu_b g_\perp B)^2)^{1/2}$ and is caused by terminteraction [11] between the two $\Gamma_{3,4}(^2E)$ doublets. The g value of the $\Gamma_4(^2T_2)$ ground state of different axial centres decreases from $g(AN1) = 0.51$ to $g(AS) = 0.29$ with increasing ZFS.

Axial centre PN. The axial PN centre has a ZFS, which is large compared with the Zeeman splitting and thus a linear Zeeman behaviour and no terminteraction in the ^2E state is observed (fig. 3). The Zeeman pattern is equivalent to the other axial centres (table 1).

2.3. *Fine structure and Zeeman effect of the Cu-blue ZPLs*

It is a striking fact that, first of all, the ZPLs of

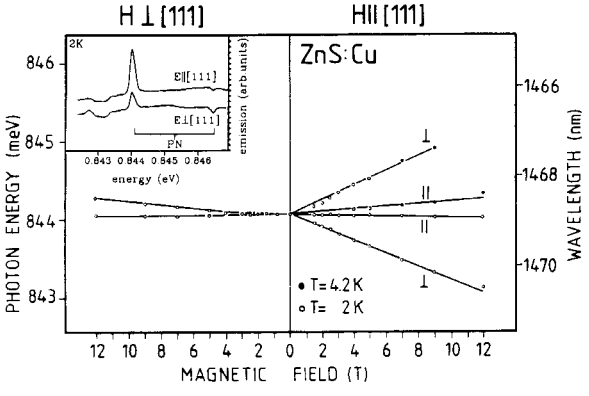

Fig. 4. Zeeman-pattern of the Cu^{2+}_{Zn} ZPLs of the PN centre for $H \parallel (1\,1\,1)$ (right) and $H \perp (1\,1\,1)$, $H \parallel (1\,1\,0)$ (left) for $T = 2$ K. The insert shows the corresponding PL spectra and the zero-field splitting in the excited ^2E state.

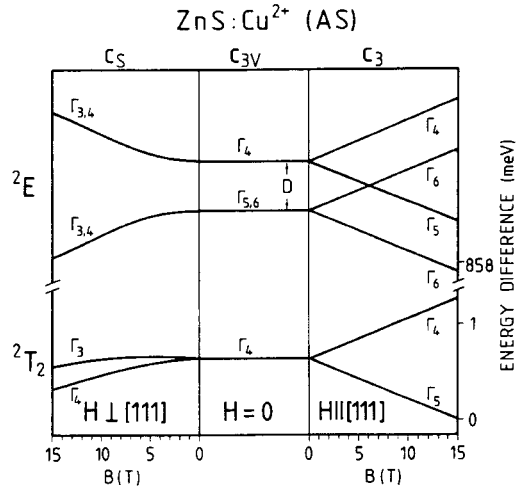

Fig. 5. Observed term scheme for the axial AS Cu^{2+}_{Zn} centre in ZnS for $H \parallel (1\,1\,1)$ (right), $H = 0$ T (middle) and $H \perp (1\,1\,1)$, $H \parallel (1\,1\,0)$ (left). This term scheme is representative for all axial Cu^{2+}_{Zn} centres in ZnS.

the Cu-blue emission at 2.965 eV do not show any influence on the polytypic crystal structure. This indicates that the related impurity centre is not a simple point defect, or that the corresponding wavefunctions are very delocalized compared with the TM wavefunctions. Secondly, the ground state of the blue emission is a singlet [12]. The excited state of the blue emission shows a ZFS of about 1 meV, but an isotropical Zeeman splitting with a g value of $g = 1.98 \pm 0.05$. A low-lying triplet and a high-energy singlet are observed in the excited state. Thus it is demonstrated that the ground as well as the excited Cu–B impurity state are no $Cu_{Zn^{2+}}$ states. Possible candidates for the Cu-related blue emission defect centre are strong coupled D–A pairs [13] or deeply bound excitions on a Cu-related defect [3,12].

3. Discussion

In section 2 an almost complete survey of all Cu_{Zn}^{2+} luminescence centres, which exists when six Zn–S layers are considered, is given for the first time. The assignments of the cubic AN centre and the hexagonal PS centre are reliable because purely cubic (and hexagonal) samples show the corresponding ZPLs. The assignments of the axial centres AS and PN, however, are not so unequivocal. Both sites have axial symmetry and should occur in equal abundance because one stacking fault creates both AS and PN sites. Due to the fact there is identical neighbourhood up to the second nearest neighbours of the impurity site of all AN and AS sites on one hand, and of all PN and PS sites on the other, a reasonable assignment can be established. The trigonal ZFS of the ^2E states of the PN and the PS centre are almost the same and agree well with the observed 1.5 meV for Cu_{Zn}^{2+} centres in hexagonal CdS [14]. The crystals contain also Fe, Ni and W. This allows the comparison of the known polytypic centres of these impurities and the observed Cu_{Zn}^{2+} centres in each single crystal. Assuming a statistical distribution of the TMs in the polymorphic ZnS crystals a crosscheck with the appearing subcentres of different TMS like Fe^{3+} [15] and Ni^{2+} [16] becomes possible in each crystal [17].

The energy shifts of the different AS, PN and PS Cu_{Zn}^{2+} defect centres compared to the cubic AN ZPL (table 1) leads to the conclusion that the empirically known superposition principle [6], which describes the influence of stacking faults on the TM energy level as a superposition of the crystal fields induced by each stacking layer, is also valid for Cu_{Zn}^{2+} centres. We get the energy of the hexagonal PS centre with the formula $E(\mathrm{AN}) + \Delta E(\mathrm{AS}) + \Delta E(\mathrm{PN}) = E(\mathrm{PS})$. The difference between the calculated and the observed energy (table 1) is small (0.14 meV).

The ZFS in the excited ^2E state and the anisotropical Zeeman splitting (fig. 5) are typical for the axial Cu_{Zn}^{2+} centres in ZnS. The small g values (down to $g = 0.28$) observed for the $\Gamma_4(^2T_2)$ ground states call for a strong Jahn–Teller effect [19]. Additionally, the centre of gravity of the $^2T_2$ state shifts to lower energies in the magnetic field (fig. 5), also indicating terminteraction with further vibronic states. The observed trends in the fine structure and the Zeeman behaviour for the differential axial distorted Cu_{Zn}^{2+} centres give new insights into the connection of the electron–phonon interaction and the trigonal crystal field. A fruitful task for the future are therefore numerical calculations, involving the spin–orbit coupling, the trigonal crystal field, the magnetic field and the Jahn–Teller effect on the same level.

Acknowledgement

The authors wish to thank Dr. R. Broser for supplying the high-quality ZnS crystals.

References

[1] K. Era, S. Shionaya and Y. Washizawa, J. Phys. Chem. Sol. 29 (1968) 1827.
[2] I. Broser, H. Maier and H.J. Schulz, Phys. Rev. A 140 (1965) 2135.
[3] M. Godlewski and K. Swiatek, J. Cryst. Growth 117 (1992) 634.
[4] I. Broser, R. Broser and E. Birkicht, J. Lumin. 40–41 (1988) 331.

[5] T. Buch, B. Clerjaud, B. Lambert and P. Kovacs, Phys. Rev. B 7 (1973) 184.
[6] U.W. Pohl, A. Ostermeier, W. Busse and H.E. Gumlich, Phys. Rev. B 42 (1990) 5751.
[7] I. Broser and R. Broser-Warminsky, Deutsches Patentamt, Patentschrift 814193 (1950).
[8] R. Heitz, A. Hoffmann, P. Thurian and I. Broser, J. Phys. C 4 (1992) 157.
[9] B. Clerjaud, Acta Phys. Pol. A 73 (1988) 909.
[10] I. Broser, U. Scherz and M. Wöhlecke, J. Lumin. 1–2 (1970) 39.
[11] P. Thurian, R. Heitz, A. Hoffmann and I. Broser, J. Cryst. Growth 117 (1992) 727.
[12] A. Hoffmann, A. Franz, A. Ismail, F. Asch and I. Broser, Mater. Sci. Forum 38–41 (1989) 525.
[13] J.J. Davies, R.T. Cox and J.E. Nicholls, Phys. Rev. B 30 (1984) 4516.
[14] A. Hoffmann, I. Broser, P. Thurian and R. Heitz, J. Cryst. Growth 101 (1990) 532; I. Broser, A. Hoffmann, R. Heitz and P. Thurian, J. Lumin. 48–49 (1991) 693.
[15] A. Hoffmann, R. Heitz and I. Broser, Phys. Rev. B 41 (1990) 5806.
[16] U. Kaufmann, P. Koidl and O.F. Schirmer, J. Phys. C 6 (1973) 310.
[17] P. Thurian, R. Heitz, A. Hoffmann and I. Broser, to be published.
[18] R.E. Dietz, H. Kamimura, M.D. Sturge and A. Yariv, Phys. Rev. 132 (1963) 1559.
[19] T. Yamaguchi and H. Kamimura, J. Phys. Soc. Japan 33 (1972) 953.